Confinement-Deconfinement Transition as an Indication of Spin-Liquid-Type Behavior in Na_2IrO_3

Zhanybek Alpichshev,[1] Fahad Mahmood,[1] Gang Cao,[2] and Nuh Gedik[1,*]
[1]Department of Physics, Massachusetts Institute of Technology, Cambridge, Massachusetts 02139, USA
[2]Department of Physics and Astronomy, University of Kentucky, Lexington, Kentucky 40506, USA
(Received 7 May 2014; published 7 January 2015)

We use ultrafast optical spectroscopy to observe binding of charged single-particle excitations (SE) in the magnetically frustrated Mott insulator Na_2IrO_3. Above the antiferromagnetic ordering temperature (T_N) the system response is due to both Hubbard excitons (HE) and their constituent unpaired SE. The SE response becomes strongly suppressed immediately below T_N. We argue that this increase in binding energy is due to a unique interplay between the frustrated Kitaev and the weak Heisenberg-type ordering term in the Hamiltonian, mediating an effective interaction between the spin-singlet SE. This interaction grows with distance causing the SE to become trapped in the HE, similar to quark confinement inside hadrons. This binding of charged particles, induced by magnetic ordering, is a result of a confinement-deconfinement transition of spin excitations. This observation provides evidence for spin liquid type behavior which is expected in Na_2IrO_3.

DOI: 10.1103/PhysRevLett.114.017203 PACS numbers: 75.10.Kt, 71.10.Li, 78.47.jj

Spin-orbit coupling (SOC) can give rise to highly nontrivial physics. Prime examples of the role of SOC in condensed matter systems are the topological insulators which have a nontrivial topology of their band structure due to sufficiently strong SOC [1,2]. In the case of simpler "band topological insulators," the gap is determined by the spin-orbit coupling and the system can be treated as noninteracting. These materials have been subject to intensive research and are relatively well understood. Much less clear is the situation in which the insulating state before the "turning on" of SOC was not a trivial band insulator but an insulator with a gap driven by electron-electron interactions, such as a Mott insulator.

Iridate compounds belong to the class of materials in which electron-electron interactions play an essential role. Expected to be metallic based on a simple electron count, these systems are insulators exhibiting Mott-type behavior. On the other hand, due to the extended nature of the $5d$ orbitals, the on-site Coulomb repulsion has a moderate value ($U \approx 0.4$–2.5 eV) and SOC ($\approx$0.4–1 eV) effectively competes with electron-electron interactions [3].

One of the most intriguing proposals of novel physics made for iridate compounds was that the interplay between spin-orbit interactions, crystal field splitting, and Coulomb repulsion of $5d$ electrons in Na_2IrO_3 can lead to a formation of effective moments with $J_{\text{eff}} = 1/2$ on every Ir-O octahedron with highly anisotropic nearest neighbor coupling. This coupling has a very special form and, given its layered quasi-2D honeycomb lattice structure, was proposed [4–7] to be a solid-state realization of the Kitaev model [8] of a spin liquid.

The real Hamiltonian of Na_2IrO_3 is, however, not a pure Kitaev model and should also have conventional terms such as Heisenberg-type exchange interaction between effective moments. Such terms generally spoil the symmetry of the pure Kitaev model and result in an ordered ground state [5,7,9] in the limit of low temperatures. The structure of the ground state should then depend on the details of the extra term in the Hamiltonian. Neutron studies [10–12] have revealed that Na_2IrO_3 has an antiferromagnetic ground state of "zigzag" type [Fig. 3(b)] with a Néel temperature of $T_N = 15.3$ K. The minimal Hamiltonian within the framework of the modified Kitaev model that can give such a ground state consists of an antiferromagnetic Kitaev term and a ferromagnetic Heisenberg term [5,7,9,13]. Although Na_2IrO_3 is not a quantum spin liquid, the fact that the ordering temperature $T_N = 15$ K is considerably smaller than both the Curie-Weiss temperature $T_\Theta = -125$ K [7] and the spin wave energy $E_{\text{sw}} \sim 5$ meV [10] implies that the degree of frustration is still quite strong and the Kitaev term should dominate the low-energy physics. Nevertheless, despite intensive research performed on Na_2IrO_3 thus far, to the best of our knowledge, there has been no evidence of the spin-liquid-type behavior in this material, which should show up in the $T_N \ll T \ll T_\Theta$ temperature range [14].

In this Letter we report our results on ultrafast studies of photoexcitations in Na_2IrO_3. We observe a change in their dynamics across Néel temperature; namely, we observe a sharp increase in the binding energy of the excitons that they form as the system enters the ordered phase. We interpret this as evidence of confinement-deconfinement transition of spin and charge excitations across T_N, which is a hallmark of spin-liquid physics [15,16].

Time-resolved experiments were performed with a Ti: sapphire oscillator lasing at the center wavelength of

 © 2015 American Physical Society

795 nm ($\hbar\omega = 1.55$ eV) producing pulses of 60 fs in duration. The repetition rate of the laser was reduced to 1.6 MHz with an external pulse picker to avoid cumulative heating effects on the sample, and the spot size of a spatially Gaussian beam was set to 60 μm FWHM. Single crystals of Na_2IrO_3 were grown using a self-flux method from off-stoichiometric quantities of IrO_2 and Na_2CO_3. Similar technical details were described elsewhere [17–19].

Data were obtained with a standard optical pump-probe technique [20,21] where a single "pump" pulse excites the sample and the resulting dynamical response is monitored by the normalized change in the reflectivity $\Delta R(t)/R$ of a separate "probe" beam as a function of time delay Δt between the pump and probe. We use the same wavelength for both pump and probe pulses. For phase-sensitive measurements a variation of the pump-probe technique called the "heterodyne transient grating" (HTG) method is used [22]. This method, unlike the pump-probe technique, can distinguish between components of ΔR with different physical origins [23]. Here an interference of two pump beams produces a spatially modulated excitation pattern which is studied by a probe beam diffracted off the sample. The diffracted beam is then heterodyned with an additional beam used as a local oscillator. The time dependence $\Delta R(t)$ of a multicomponent system response obtained in this way changes as a function of the phase difference ϕ between the probe beam and the local oscillator, whereas that of a single-component system just scales proportionally to $\cos(\phi)$ (also see the Supplemental Material [24]).

Given the band structure of Na_2IrO_3 [26–28] [Fig. 1(a)], the absorption of a pump photon with energy E eV causes electrons to transition from a $J_{\text{eff}} = 3/2$ band into the upper Hubbard band, which is the only accessible level for the excited electrons for this photon energy. The depleted valence band is then partially refilled through relaxation of the photoexcited electrons and partially with electrons from the lower Hubbard band [Fig. 1(a)]. At the end of this relatively fast process the system will have some amount of excitations in the upper Hubbard band (double occupancies in real space or "doublons") and an equal amount of holes in the lower Hubbard band. The excited state is metastable as the optical dipole transitions within the Hubbard band are prohibited by selection rules ($\Delta J = 0$ transition). Moreover, the energy of the magnons, which are the relevant excitations $\epsilon \approx 5$–10 meV $\sim k_B T_\Theta$ [10], is much less than the Hubbard gap $U \sim 350$ meV, which is the energy which needs to be dissipated during the doublon-hole recombination process, making the lifetime exponentially large in U/ϵ [29]. This observation allows us to consider holes and doublons as stable quasiparticles for the time scales relevant to our experiments (~100 ps).

Figures 1(b) and 1(c) show HTG data taken at a pump fluence of ~9.5 μJ/cm^2 for various values of ϕ at 295 and 25 K, respectively. At each temperature the shape of the differential reflectivity time trace $\Delta R(t)/R$ with time changes as ϕ is varied, indicating that there is more than one component in the system response. This behavior is in agreement with earlier resonant inelastic x-ray scattering (RIXS) studies [26,30], which demonstrated that the low-energy excitations of Na_2IrO_3 are single-particle (doublons and holes) excitations (SE) and their bound state is known as a Hubbard exciton (HE) [31]. Figures 3(a) and 3(b) demonstrate that the component featuring the fast spike near $t = 0$ is clearly getting stronger with increasing temperature, allowing us to identify it with SE. This is similar to the results of studies of photoexcited Mott insulators in other systems [31] where the $\Delta R/R$ component with an initial fast spike was shown to be due to SE whereas the one without is due to HE.

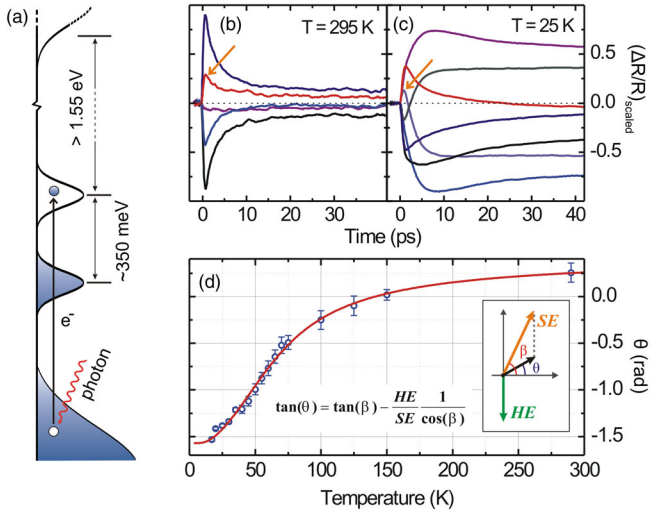

FIG. 1 (color online). (a) Sketch of the band structure of Na_2IrO_3 illustrating the relevant processes during photoexcitation with 1.5 eV light. (b) HTG traces for selected values of ϕ (see text) at a pump fluence of 9.5 μJ/cm^2 at $T = 295$ K and (c) at $T = 25$ K. Note the multicomponent behavior of the HTG traces as a function of ϕ and the relative strengthening of the initial spike (labeled with an arrow) associated with single-particle excitations (SE) at higher temperature (see text). (d) Phase (θ) of the total signal at $t \approx 50$ ps in the quasiequilibrium state as a function of temperature. Error bars represent the 95% confidence interval (2 s.d.) in extracting the phase. Solid red line is a fit to the data based on the Boltzmann distribution of SE and Hubbard exciton (HE) populations, $\text{SE/HE} \propto \exp(-\Delta/k_B T)$. Inset: Phasor diagram representing quasiequilibrium ΔR (black phasor) due to SE and HE.

It should be noted that both components (SE and HE) are long-lived and thus they both contribute to the composition of the total signal in the long-time limit. There, a quasi-thermal equilibrium is established between SE and HE and thus their population ratio should be proportional to the Boltzmann factor $\exp(-\Delta/k_B T)$, where Δ is the HE binding energy. In this regime, the net phase θ of the signal response reaches a constant value that is directly related to the quasiequilibrium population ratio of SE and HE (see

the inset of Fig. 1(d) and the Supplemental Material [24]). This phase θ is plotted in Fig. 1(d) as a function of temperature from which we extract $\Delta \approx 4.6 \pm 0.8$ meV. This value is within the bounds set by RIXS measurements [26] and confirms that the component featuring a fast spike at $t = 0$ is indeed due to SE. Figures 2(a) and 2(b) show the HTG data taken for a very low pump fluence of value of ~ 30 nJ/cm^2 at temperatures above and below T_N, respectively. Similar to the higher fluence data, the low fluence response above T_N [Fig. 2(a)] clearly features more than one component, indicating the presence of both SE and HE. On the other hand, the low fluence response below T_N [Fig. 2(b)], strikingly, scales proportionally to $\cos(\phi)$, implying a single-component behavior, which, as discussed above, is due to Hubbard excitons.

We now proceed to study this disappearance of SE as a function of temperature by performing optical pump-probe measurements for low excitation densities to minimize heating effects. Figure 2(d) shows reflectivity transients for various temperatures below T_N for two different pump fluences. As can be seen, the normalized system response

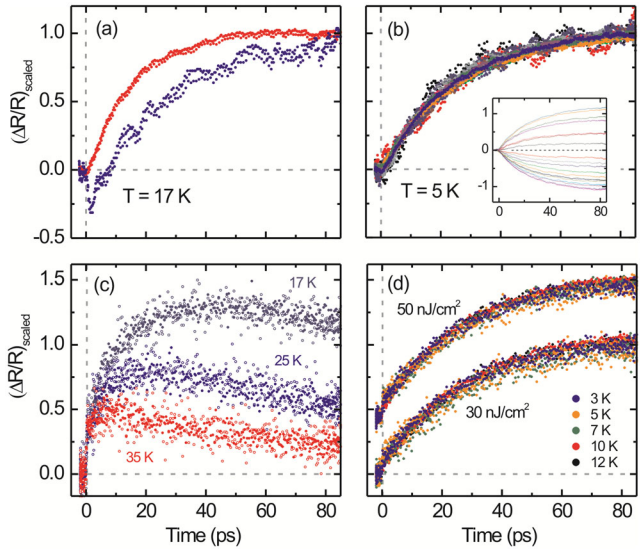

FIG. 2 (color online). HTG and pump-probe data at various temperatures at low pump fluence. (a) Representative HTG traces at $T = 17$ K for two different values of ϕ at a pump fluence of 30 nJ/cm^2. The traces exhibit qualitatively different shapes indicating the presence of both SE and HE. Note the fast spike around $t = 0$ for the purple curve. This is signature of SE (see Fig. 1 and text). (b) HTG traces at $T = 5$ K for 19 different values of ϕ at a pump fluence of 30 nJ/cm^2, scaled to emphasize the single component (HE) nature of the response. Inset: Unscaled HTG traces. (c) Scaled $\Delta R/R$ traces for temperatures above T_N ($T = 17$, 25, and 35 K) at different fluences: 100 nJ/cm^2 (filled markers) and 50 nJ/cm^2 (open markers). Note the strong temperature dependence and the lack of fluence dependence in this limit. (d) $\Delta R/R$ traces for temperatures below T_N ($T = 5$, 7, 10, and 12 K), scaled to emphasize the universal behavior of transient traces. Upper curve, 50 nJ/cm^2; lower curve, 30 nJ/cm^2. Curves at different fluence values are shifted for better clarity.

in this regime is independent of both temperature and pump fluence, demonstrating that the single-component behavior observed at $T = 5$ K persists up to T_N. This indicates that SEs are suppressed throughout the ordered phase. On the contrary, reflectivity transients above T_N [Fig. 2(c)] strongly depend on temperature, which combined with the HTG data (Fig. 1) indicate the formation and strengthening of the component due to SE. Moreover, above T_N, the normalized transients at each temperature are independent of pump fluence [Fig. 2(c)], demonstrating that the relative composition of the signal (ratio between SE and HE populations) is constant as a function of pump fluence in this low excitation density regime. This sudden disappearance of SE at T_N implies a sharp increase in the HE binding energy.

In general, an increase in binding energy of an exciton can be either due to an enhancement of the attracting potential or due to "slowing down" of the overall dynamics, e.g., by increasing the effective mass. The effective mass of a single hole in a Mott insulator is indeed enhanced due to emission of magnons, but this happens in both the antiferromagnetic and disordered phases [32]. But more importantly, it is the sheer disparity between the bandwidth of the single-particle excitations ($\gtrsim 100$ meV, e.g., Ref. [26]) and the Heisenberg coupling responsible for antiferromagnetism ($\sim k_B T_N \approx 1$ meV) that makes the slowing-down scenario unlikely. Therefore, we conclude that the increase in binding energy of HE is a result of enhancement in attraction between SEs.

Here we present a simple intuitive picture of the effective attraction mediated by antiferromagnetic ordering responsible for additional binding energy, based on the Kitaev-Heisenberg model. This Hamiltonian naturally gives rise to the zigzag order [9]:

$$H_{\mathrm{KH}} = J_K \sum_{\langle ij \rangle} S_i^l S_j^l + J_H \sum_{\langle ij \rangle} \vec{S}_i \cdot \vec{S}_j. \qquad (1)$$

The main term here is the strongly frustrated Kitaev term ($T_\Theta = -125$ K). The Heisenberg term lifts the degeneracy and the system "freezes" into an ordered state below T_N. In the zigzag phase every spin finds its "Kitaev partner" and antialigns itself with the spin of its partner in the direction determined by the orientation of the connecting bond. The much smaller Heisenberg term ($T_N = 15.3$ K) tries to minimize its energy under the condition that every spin has a Kitaev partner. As can be seen in Fig. 3(b), the zigzag order satisfies this condition for all bonds except those that connect Kitaev partners.

This situation changes drastically when spinless defects such as doublons or holes are introduced into the system. These particles can be thought of as topological in the same sense as the excitations in the Rokhsar-Kivelson dimer model [33]. The spins that have lost their Kitaev partners reorganize the surrounding spin order at the expense of Heisenberg energy [Fig. 3(c)]. Reoriented spins form a

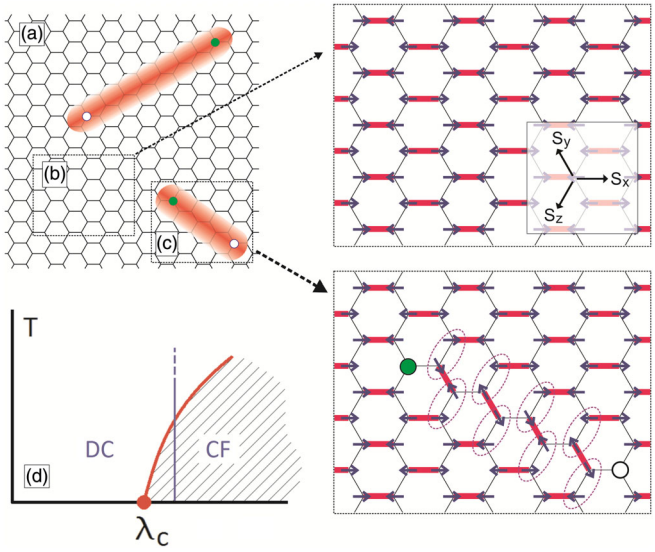

FIG. 3 (color online). (a) Schematic view of an excited sample. Green dots correspond to doublons while the white dots represent holes. The shaded red area marks the region where the spins are affected by the reconstruction, i.e., the "string" [see (c)]. (b) Sketch representing the zigzag ordered low temperature ground state. Red bonds connect Kitaev partners while gray bonds have a spin configuration that minimizes the Heisenberg energy. (c) Simplified representation of the restructured state with singlet defects (hole or doublon). The Heisenberg energy along the bonds highlighted by purple ovals is no longer minimal. The string composed of such bonds must begin and end on a defect. (d) Illustration of a phase diagram of a modified Kitaev model with a first-order quantum critical point and a phase boundary between confined (CF) and deconfined (DC).

string terminating on the other defect. The energy cost of this configuration is proportional to the number of broken Heisenberg links, which in turn is proportional to the length of the string connecting the two defects. This prohibits the long-range separation of the defects which, in the case of low excitation density, will predominantly be of opposite charges (doublon-hole), leading to an enhanced binding between them in addition to Coulomb attraction. This is similar to the picture of the quark confinement in high-energy physics [34]: separation of defects produces a string of perturbed vacuum between them with an energy proportional to its length. However, since breaking of this string in our case produces a pair of electrically neutral unpaired "dangling" spins (which *are* confined), the binding energy between doublons and holes is limited by the cost of breaking a Kitaev pair, which is of the order of Kitaev coupling, $J_K \approx 10$ meV in the case of Na_2IrO_3.

This is consistent with previous theoretical works on the Kitaev-Heisenberg model where it was observed that for sufficiently weak perturbations the Kitaev spin-liquid state persists, but as the extra term gets stronger, the system enters an ordered state [4,5,35]. Formulated in terms of spinons, such a transtition corresponds to the transition from a deconfined state (spin-liquid) to a confined state (antiferromagnet) [35,36]. This is a first-order phase transition [35,36], and no quantum critical region is expected above the quantum critical point $\lambda = \lambda_c$ [37], where λ is the relative strength of the Heisenberg term in the Hamiltonian. Therefore, confined and deconfined phases are separated by a simple boundary and the confinement-deconfinement transition can be observed not only by tuning the strength of the perturbing term λ at $T = 0$ as in Refs. [35,36], but also by going across the ordering temperature for a fixed $\lambda > \lambda_c$ [see Fig. 3(d)]. In the confined phase, all fractional excitations such as holons, doublons, and spinons are bound to each other and, conversely, can move independently in the deconfined phase [16].

The fact that the zigzag order is not a trivial antiferromagnet was evidenced in a recent work of Manni *et al.* [38], where partial substitution of Ir atoms with nonmagnetic Ti atoms resulted in the formation of a spin glass state at low temperatures. This has a natural explanation within our framework, as Ti sites can be treated as static spinless defects. At sufficient concentration they will be connected by spin strings as in Fig. 2(c). Since there are many different ways to connect different Ti sites, it is natural to expect a spin glass state at low temperatures.

In conclusion, we performed an optical pump-probe study of Na_2IrO_3, a material proposed to be a realization of the Kitaev model. We observed that photoinduced charged excitations display drastically different behavior below and above the Néel ordering temperature. Namely, the binding energy of the excitons that these particles form undergoes a sharp increase upon entering the ordered phase. Based on earlier theoretical studies on doped Mott insulators, we conjecture that this is due to an effective attraction brought about by the antiferromagnetic order rather than because of an increase in effective mass of quasiparticles. We argue that this attraction is a manifestation of confinement of spin excitations anticipated in the ordered phase of the Kitaev-Heisenberg model. Therefore, the change of behavior that we observe at the Néel temperature is due to the confinement-deconfinement transition, providing evidence of spin-liquid-type physics in Na_2IrO_3.

We thank Senthil Todadri, Patrick Lee, Subir Sachdev, and Maksym Serbyn for insightful discussions. This work was supported by the Army Research Office Grant No. W911NF-11-1-0331 (data taking and analysis), NSF Career Award No. DMR-0845296 (experimental setup), and the Alfred P. Sloan Foundation (theory and modeling). G. C. was supported by NSF Grants No. DMR-0856234 and No. DMR-1265162 (material growth).

*gedik@mit.edu

[1] M. Z. Hasan and C. Kane, Rev. Mod. Phys. **82**, 3045 (2010).
[2] X.-L. Qi and S.-C. Zhang, Rev. Mod. Phys. **83**, 1057 (2011).

[3] F. Ye, S. Chi, H. Cao, B. C. Chakoumakos, J. A. Fernandez-Baca, R. Custelcean, T. F. Qi, O. B. Korneta, and G. Cao, Phys. Rev. B **85**, 180403(R) (2012).
[4] G. Jackeli and G. Khaliullin, Phys. Rev. Lett. **102**, 017205 (2009).
[5] J. Chaloupka, G. Jackeli, and G. Khaliullin, Phys. Rev. Lett. **105**, 027204 (2010).
[6] Y. Singh and P. Gegenwart, Phys. Rev. B **82**, 064412 (2010).
[7] Y. Singh, S. Manni, J. Reuther, T. Berlijn, R. Thomale, W. Ku, S. Trebst, and P. Gegenwart, Phys. Rev. Lett. **108**, 127203 (2012).
[8] A. Kitaev, Ann. Phys. (Amsterdam) **321**, 2 (2006).
[9] J. Chaloupka, G. Jackeli, and G. Khaliullin, Phys. Rev. Lett. **110**, 097204 (2013).
[10] S. K. Choi *et al.*, Phys. Rev. Lett. **108**, 127204 (2012).
[11] X. Liu, T. Berlijn, W.-G. Yin, W. Ku, A. Tsvelik, Y.-J. Kim, H. Gretarsson, Y. Singh, P. Gegenwart, and J. P. Hill, Phys. Rev. B **83**, 220403 (2011).
[12] F. Ye, S. Chi, H. Cao, B. C. Chakoumakos, J. A. Fernandez-Baca, R. Custelcean, T. F. Qi, O. B. Korneta, and G. Cao, Phys. Rev. B **85**, 180403 (2012).
[13] J. G. Rau, E. Kin-Ho Lee, and H. Y. Kee, Phys. Rev. Lett. **112**, 077204 (2014).
[14] L. Balents, Nature (London) **464**, 199 (2010).
[15] S. Sachdev, Rev. Mod. Phys. **75**, 913 (2003).
[16] T. Senthil and M. P. A. Fisher, J. Phys. A **34**, L119 (2001).
[17] M. Ge, T. F. Qi, O. B. Korneta, D. E. De Long, P. Schlottmann, W. P. Crummett, and G. Cao, Phys. Rev. B **84**, 100402(R) (2011).
[18] S. Chikara, O. Korneta, W. Crummett, L. DeLong, P. Schlottmann, and G. Cao, Phys. Rev. B **80**, 140407(R) (2009).
[19] M. A. Laguna-Marco, D. Haskel, N. Souza-Neto, J. C. Lang, V. V. Krishnamurthy, S. Chikara, G. Cao, and M. van Veenendaal, Phys. Rev. Lett. **105**, 216407 (2010).
[20] J. Demsar, K. Biljakovic, and D. Mihailovic, Phys. Rev. Lett. **83**, 800 (1999).
[21] G. Segre, N. Gedik, J. Orenstein, D. Bonn, R. Liang, and W. Hardy, Phys. Rev. Lett. **88**, 137001 (2002).
[22] N. Gedik and J. Orenstein, Opt. Lett. **29**, 2109 (2004).
[23] J. P. Hinton, J. D. Koralek, Y. M. Lu, A. Vishwanath, J. Orenstein, D. A. Bonn, W. N. Hardy, and R. Liang, Phys. Rev. B **88**, 060508(R) (2013).
[24] See Supplemental Material at http://link.aps.org/supplemental/10.1103/PhysRevLett.114.017203, which includes [25], for more details on the experimental technique and sample preparation; and also includes additional arguments supporting main conclusions of the paper along with further discussion relevant to the physical picture presented in this Letter.
[25] G. M. Sheldrick, Acta Crystallogr. Sect. A **64**, 112 (2008).
[26] H. Gretarsson *et al.*, Phys. Rev. Lett. **110**, 076402 (2013).
[27] R. Comin *et al.*, Phys. Rev. Lett. **109**, 266406 (2012).
[28] C. H. Sohn *et al.*, Phys. Rev. B **88**, 085125 (2013).
[29] R. Sensarma, D. Pekker, E. Altman, E. Demler, N. Strohmaier, D. Greif, R. Jördens, L. Tarruell, H. Moritz, and T. Esslinger, Phys. Rev. B **82**, 224302 (2010).
[30] H. Gretarsson *et al.*, Phys. Rev. B **87**, 220407 (2013).
[31] F. Novelli, D. Fausti, J. Reul, F. Cilento, P. H. M. van Loosdrecht, A. A. Nugroho, T. T. M. Palstra, M. Gruninger, and F. Parmigiani, Phys. Rev. B **86**, 165135 (2012).
[32] C. L. Kane, P. A. Lee, and N. Read, Phys. Rev. B **39**, 6880 (1989).
[33] S. A. Kivelson, D. S. Rokhsar, and J. P. Sethna, Phys. Rev. B **35**, 8865 (1987).
[34] A. M. Polyakov, *Gauge Fields and Strings* (Harwood, Academic, Chur, Switzerland, 1987).
[35] R. Schaffer, S. Bhattacharjee, and Y. B. Kim, Phys. Rev. B **86**, 224417 (2012).
[36] S. Mandal, S. Bhattacharjee, K. Sengupta, R. Shankar, and G. Baskaran, Phys. Rev. B **84**, 155121 (2011).
[37] S. Sachdev, Nat. Phys. **4**, 173 (2008).
[38] S. Manni, Y. Tokiwa, and P. Gegenwart, Phys. Rev. B **89**, 241102(R) (2014).